**ATLAS NOTE**

August 4, 2015

# Trigger studies for LHC Run-2 $W' \to tb \to qqbb$ search

D. Wilbern[a] and J. Love[b]

[a]*Department of Physics, Northern Michigan University, 1401 Presque Isle Ave, Marquette, MI 49855, USA*
[b]*HEP Division, Argonne National Laboratory, 9700 S. Cass, Argonne, IL 60439, USA*

**Abstract**

A preliminary study of usable triggers for the Run-2 $W' \to tb$ search in the hadronic final state is presented. QCD dijet events generated by Pythia are used to investigate how systematic uncertainty of background estimation is affected by the choice of trigger. Choosing more restrictive triggers will reduce background rates, but will also increase the lower bound on the mass range of $W'$particles the search is sensitive to. Single jet $p_T$ triggers, $H_T$ triggers, multijet $p_T$ triggers, b-tag triggers, and proposed $H_T$+ b-tag triggers are investigated in this study. For each trigger investigated, the lower bound of the acceptable $W'$ invariant mass range as well as the tagging efficiency ratios are presented.

# 1 Introduction

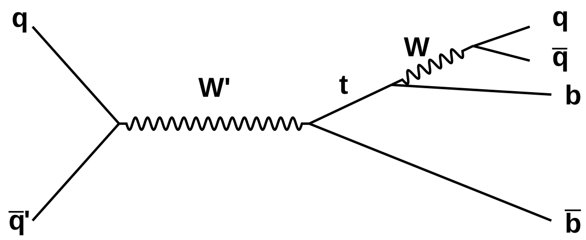


Figure 1: $W' \to tb$ Feynman diagram in the hadronic decay channel.

Many "Beyond the Standard Model" theories, particularly those that involve SU(2) gauge symmetries, predict the existence of new heavy gauage bosons called $W'$ bosons. LHC Run-1 analyses at $\sqrt{s} = 8$ TeV searched for $W'$ decaying into a top quark and a bottom quark[1]. These analyses excluded $W'$ bosons in the top quark leptonic decay channel ($W' \to \ell\nu$) and hadronic decay channel ($W' \to tb \to qqbb$) below 1.7 TeV and 1.5 TeV, respectively, at a 95% confidence level[1][2]. $W' \to tb$ in this note will henceforth refer to the $W'$ search in the all hadronic final state, $W' \to tb \to qqbb$. The Feynman diagram for this state is shown in Figure 1.

QCD dijet events generated by Pythia are used in this study to investigate the lower-bound on the acceptable range of background events' $m_{tb}$. $W' \to tb$ events are dijet events with a large-$R$ jet top-tagged and a high-$p_T$ small-$R$ jet b-tagged. QCD multijet events provide the highest background contribution by far: about 99%. Contribution from $qq \to W^+ \to t\bar{b}$ can be reduced with a low-end energy cut, and contribution from other QCD multijet events can be reduced with flavor-tagging requirements. These requirements improve the ratio in cross-sections of background events to signal events from $O(10^6)$ to $O(10^1)$[3]. The ATLAS trigger system will be used to apply the energy requirement, the $W'$ top-tagger[2] is used to tag top jets, and a neural-network based algorithm is used to tag b-jets.

Figure 2 shows data[2] from the Run-1 hadronic state analysis fitted to the expected background distribution. A more restrictive event trigger would not reach its trigger plateau until a higher value of $m_{tb}$ than the one here, resulting in a need to shift the left-edge of the plot to the right, meaning a loss of sensitivity to signals at lower $m_{tb}$. This study is a preliminary investigation of triggers proposed for use in the Run-2 $W' \to tb$ search, with the intent of maximizing the $m_{tb}$ range the analysis is sensitive in.

[1] The decays $W'^+ \to t\bar{b}$ and $W'^- \to \bar{t}b$ are both equally considered. For simplicity this document refers to both as $W' \to tb$.

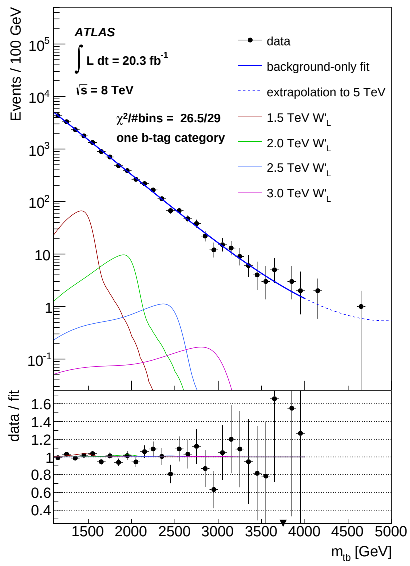


Figure 2: Data from the run 1 $W'$ search fitted to a four-parameter function.

# 2 Study Approach

## 2.1 Trigger Turn-on Curves

Trigger efficiency curves, or "turn-on" curves, were made for the triggers being investigated in this study. A trigger's efficiency is determined by dividing a quantity such as leading jet $p_T$ for events passing the trigger by the same quantity for all events. These efficiencies were plotted as a function of leading small-$R$ jet $p_T$, leading large-$R$ jet $p_T$, small-$R$ jets' $H_T$, and large-$R$ jets' $H_T$. These curves can be found in Appendix A. Sample turn-on curves for the three triggers HLT_ht700, HLT_ht850, and HLT_ht1000 are shown in figure 3. The "trigger plateau" region is taken as the region where 95% or more of events pass the trigger. Note that the trigger plateau region begins at higher values on the x-axis for more restrictive triggers. A trigger's behavior is stable in this region, so background contribution can be investigated without introducing bias from the trigger, For this reason we use the trigger plateau region for the efficiency curves to determine the minimum $p_T$ cut for the event categorization routine in Section 2.2. For each trigger we choose the start of the trigger plateau from either the small-$R$ jet $p_T$ turn-on curve or the large-$R$ jet $p_T$ turn-on curve, whichever has the higher value.

The MC data used in this study was binned into ten samples by $p_T$ of the leading parton at truth level. The events in these samples are weighted on per-sample basis and for some samples a per-event basis also. To generate the trigger turn-on curves, the per-sample weights were applied, but not the per-event weights because the weighting scheme was found to be inappropriate for generating turn-on curves as a function of leading-jet $p_T$. As a result, the "stegosaurus" shape exhibited by some of the turn-on curves remains as an artifact of this weighting. The x-axis location of the spikes correspond to the $p_T$ binning of the MC samples. Some triggers, in particular two of the b-tag triggers and a multijet trigger, had low statistics and it is probably not appropriate to draw conclusions about them based on the results of this study.

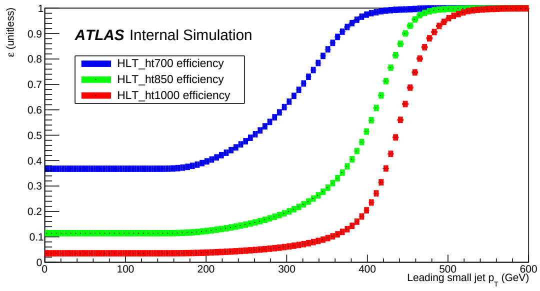


Figure 3: Some sample trigger turn-on curves, see appendix A for more. The trigger plateau starts later on the x-axis for more restrictive triggers.

### 2.2 Event Categorization and Jet Selection

A $W' \to tb$ event takes the form of a top-tagged $R$=1.0 anti-kt jet and a b-tagged high-$p_T$ $R$=0.4 anti-kt jet. We require that jets pass jet cleaning level MediumBad. We also require for the large-$R$ jet $|\eta| < 2.0$ and for the small R jet $|\eta| < 2.5$, and $\Delta R < 2.0$ between the two jets. There is also a minimum $p_T$ requirement that is chosen as the low-end of the trigger plateau region for the trigger being studied, rounded up in multiples of 50 GeV. This $p_T$ requirement is allowed to be in the range 350 GeV - 800 GeV. See Section 2.1 for details. Events without jets that meet these requirements are rejected and not considered in the background estimation.

A data-driven method called the ABCD method is used to estimate the background distribution in the signal region. Events failing the top-tagging requirement and/or the b-tagging requirement are classified as belonging to one of the control regions: A, B, or C. The orthogonality of the tagging requirements then allows the control regions to be used to estimate the contribution of background in the signal region, D. This estimation is calculated as $D = \frac{B \times C}{A}$. Figure 4 details the criteria for the event classification and the algorithm for classifying a dijet event into one of these regions while selecting the representative large-$R$ and small-$R$ jets.

The actual $m_{tb}$ distribution of events classified in region D is compared to the ABCD method's prediction. Since we are using QCD dijet events, the signal region is dominated by background too, so the two distributions should agree well. These comparisons can be found in Appendix B. The left edge of the X-axis is determined by adding 1200 GeV to the start of the lower trigger leading $p_T$ plateau threshold for that trigger.

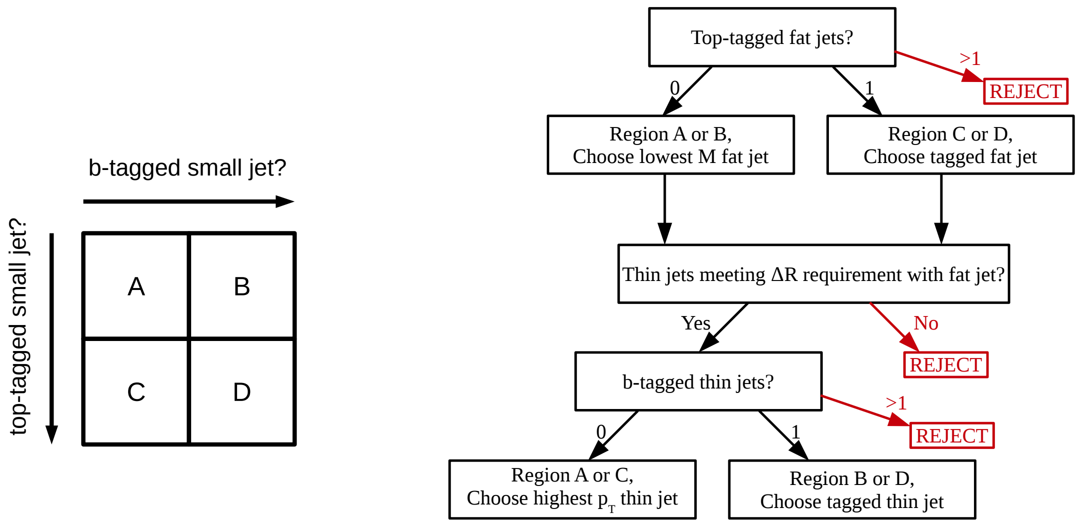


Figure 4: Event classification with the ABCD method. All jets must pass jet cleaning, min. $p_T$ and max. $|\eta|$ requirements before being considered for selection.

# 3 Trigger Study

## 3.1 Triggers Investigated

This study was performed to investigate the impact of trigger choice on the Run-2 $W' \to tb$ hadronic final state analysis. Table 1 lists the triggers we selected for this study. In addition to these, we investigated the possibility of an $H_T$ + b-tag trigger. Events that pass an $H_T$ trigger and a less restrictive b-tagging requirement are deemed to pass this $H_T$ + b-tag trigger.

Table 1: List of triggers selected for study.

| Single jet | $H_T$ | B-tag | Multijet |
|---|---|---|---|
| HLT_j15 | HLT_ht400 | HLT_j300_bloose | HLT_7j45 |
| HLT_j85 | HLT_ht550 | HLT_j225_bloose | HLT_6j45 |
| HLT_j400 | HLT_ht700 | HLT_j175_bmedium | HLT_5j85 |
| HLT_j460 | HLT_ht850 | HLT_2j65_btight_j85 | HLT_4j100 |
| | HLT_ht1000 | | HLT_3j175 |

## 3.2 Lower $m_{tb}$ Limit

We generated efficiency curves were produced for each trigger being studied, and then determined the start of the plateau for both of the leading jet $p_T$ turn-on curves. From these, we determined the lowest acceptable $m_{tb}$ for each trigger as $(1200\text{ GeV} + \mathit{AK4\ plateau\ start})$. These values can be found in Table 2.

Table 2: Start of trigger plateaus for leading-$p_T$ turn-on curves, and lowest acceptable $m_{tb}$.

| Trigger | Ak4 plateau start [GeV] | Ak10 plateau start [GeV] | Lowest $m_{tb}$ |
|---|---|---|---|
| No trigger | 350 | 350 | 1550 |
| HLT_j400 | 450 | 650 | 1650 |
| HLT_j460 | 500 | 700 | 1700 |
| HLT_j85 | 350 | 350 | 1550 |
| HLT_j15 | 350 | 350 | 1550 |
| HLT_ht400 | 350 | 350 | 1550 |
| HLT_ht550 | 350 | 350 | 1550 |
| HLT_ht700 | 400 | 450 | 1600 |
| HLT_ht850 | 450 | 500 | 1650 |
| HLT_ht1000 | 500 | 550 | 1700 |
| HLT_j300_bloose | 600 | 550 | 1800 |
| HLT_j225_bloose | 800 | 800 | 2000 |
| HLT_j175_bmedium | 400 | 450 | 1600 |
| HLT_2j65_btight_j85 | 350 | 350 | 1550 |
| HLT_7j45 | 350 | 500 | 1550 |
| HLT_6j45 | 350 | 500 | 1550 |
| HLT_5j85 | 550 | 500 | 1750 |
| HLT_4j100 | 550 | 500 | 1750 |
| HLT_3j175 | 650 | 550 | 1850 |
| "B-tag" | 350 | 350 | 1550 |
| "HLT_ht400 + B-tag" | 350 | 350 | 1550 |
| "HLT_ht550 + B-tag" | 350 | 350 | 1550 |
| "HLT_ht700 + B-tag" | 400 | 450 | 1600 |
| "HLT_ht850 + B-tag" | 450 | 500 | 1650 |
| "HLT_ht1000 + B-tag" | 500 | 500 | 1700 |

### 3.3 Ratio of Tagging Efficiencies

An important part of this study is to identify whether the triggers introduce bias into the top-tagging and b-tagging requirements. If the tagging requirements are not orthogonal, then the ABCD method cannot be used to estimate background contribution in the signal region. In order to investigate how orthogonal the tagging requirements are to each other, we calculated and compared tagging efficiencies across the borders of the different ABCD regions.

We define tagging efficiencies as:

$$\varepsilon_b = \frac{B}{A+B};\ \varepsilon_t = \frac{C}{A+C};\ \varepsilon_{bt} = \frac{D}{A+B+C+D}$$

where $\varepsilon_b$ is the efficiency to b-tag, $\varepsilon_t$ is the efficiency to top-tag, and $\varepsilon_{bt}$ is the efficiency to both b-tag and top-tag. $A$, $B$, $C$, and $D$ are the total number of events categorized in that region by the ABCD method. These efficiencies are related by:

$$\varepsilon_b \varepsilon_t = f_c \varepsilon_{bt}$$

where $f_c$ is a coefficient that describes the correlation of the tagging efficiencies. It should be close to 1 for uncorrelated tagging requirements.

We also compared the values of efficiency to b-tag across the borders of regions A and B as well as regions C and D. We define:

$$\varepsilon_{b1} = \frac{B}{A+B};\ \varepsilon_{b2} = \frac{D}{C+D}$$

where $\varepsilon_{b1}$ is the efficiency to b-tag across the region A-B border and $\varepsilon_{b2}$ is the efficiency to b-tag across the region C-D border. These efficiencies are related by:

$$\varepsilon_{b1} = f_c \varepsilon_{b2}$$

where $f_c$ is a coefficient that describes how correlated the b-tag requirement is to whether or not there was a top-tag. This value should be close to 1 if there is no correlation.

Similarly, we define:

$$\varepsilon_{t1} = \frac{C}{A+C};\ \varepsilon_{t2} = \frac{D}{B+D}$$

where $\varepsilon_{t1}$ the efficiency to top-tag across the region A-C border and $\varepsilon_{t2}$ is the efficiency to top-tag across the region B-D border. These efficiencies are related by:

$$\varepsilon_{t1} = f_c \varepsilon_{t2}$$

where again, the correlation coefficient $f_c$ should be close to 1 to indicate no correlation.

Table 3 lists these $f_c$ values when the different triggers are applied. Values that deviate from 1 more than 10% are suffixed with a "!". To get more of a sense for the statistical uncertainty, we also calculate $\frac{\sqrt{N_D}}{N_D}$ where $N_D$ is the number of events in region D, for each trigger and scale to the value for when no trigger is applied.

To ensure that these ratios' closeness to 1 comes from bias in the tagging requirements, we repeated the ABCD method but with both tagging requirements replaced with a simple random 50% chance for each jet to pass or fail. These tagging requirements should definitely be uncorrelated and should result in an $f_c$ value close to 1, so any deviation from 1 can be taken as the fractional uncertainty due to Monte Carlo statistics. These coefficients are given in Table 4.

Table 3: tagging efficiency correlation constants for real tagging.

| Trigger | $f_c$ | B-tagging $f_c$ | Top-tagging $f_c$ | Scaled $\frac{\sqrt{N_D}}{N_D}$ |
|---|---|---|---|---|
| No Trigger | 0.975355 | 0.977014 | 0.975966 | 1 |
| HLT_j400 | 0.996143 | 0.996557 | 0.996231 | 1.04422 |
| HLT_j460 | 0.945653 | 0.951759 | 0.946896 | 1.04977 |
| HLT_j85 | 0.975355 | 0.977014 | 0.975966 | 1 |
| HLT_j15 | 0.975355 | 0.977014 | 0.975966 | 1 |
| HLT_ht400 | 0.975355 | 0.977014 | 0.975966 | 1 |
| HLT_ht550 | 0.975355 | 0.977014 | 0.975966 | 1 |
| HLT_ht700 | 1.06669 | 1.06139 | 1.06508 | 1.01651 |
| HLT_ht850 | 0.996872 | 0.997148 | 0.996943 | 1.0236 |
| HLT_ht1000 | 1.05709 | 1.05172 | 1.05576 | 1.0297 |
| HLT_j300_bloose | 1.06917 | 1.06301 | 1.06204 | 1.46776 |
| HLT_j225_bloose | 0.786452! | 0.807185! | 0.807068! | 1.50283 |
| HLT_j175_bmedium | 1.14166! | 1.13142! | 1.11264! | 2.0892 |
| HLT_2j65_btight_j85 | 4.06371! | 3.20732! | 3.10619! | 15.6666 |
| HLT_7j45 | 0.747129! | 0.813747! | 0.751114! | 4.22229 |
| HLT_6j45 | 1.26336! | 1.19898! | 1.2565! | 2.51391 |
| HLT_5j85 | 1.33767! | 1.23807! | 1.33028! | 2.54692 |
| HLT_4j100 | 1.11289! | 1.08839 | 1.11076! | 1.73526 |
| HLT_3j175 | 1.10218! | 1.08426 | 1.0999 | 1.44365 |
| ”B-tagging” | 1.41157! | 1.37876! | 1.33684! | 1 |
| HLT_ht400 + ”B-tagging” | 1.41157! | 1.37876! | 1.33684! | 1 |
| HLT_ht550 + ”B-tagging” | 1.41157! | 1.37876! | 1.33684! | 1 |
| HLT_ht700 + ”B-tagging” | 1.51886! | 1.47003! | 1.43221! | 1.01651 |
| HLT_ht850 + ”B-tagging” | 1.46616! | 1.41568! | 1.39414! | 1.0236 |
| HLT_ht1000 + ”B-tagging” | 1.47468! | 1.42333! | 1.40097! | 1.0236 |

Table 4: tagging efficiency correlation constants for random tagging.

| Trigger | $f_c$ | B-tagging $f_c$ | Top-tagging $f_c$ | Scaled $\frac{\sqrt{N_D}}{N_D}$ |
|---|---|---|---|---|
| No trigger | 1.01805 | 1.00905 | 1.01349 | 1 |
| HLT_j400 | 1.00086 | 1.00041 | 1.00065 | 1.05469 |
| HLT_j460 | 0.988465 | 0.994564 | 0.991161 | 1.06679 |
| HLT_j85 | 1.01805 | 1.00905 | 1.01349 | 1 |
| HLT_j15 | 1.01805 | 1.00905 | 1.01349 | 1 |
| HLT_ht400 | 1.01805 | 1.00905 | 1.01349 | 1 |
| HLT_ht550 | 1.01805 | 1.00905 | 1.01349 | 1 |
| HLT_ht700 | 1.02997 | 1.01512 | 1.02221 | 1.01638 |
| HLT_ht850 | 1.00227 | 1.00113 | 1.0017 | 1.02529 |
| HLT_ht1000 | 0.97973 | 0.989931 | 0.984729 | 1.03214 |
| HLT_j300_bloose | 0.967832 | 0.98426 | 0.975731 | 2.56099 |
| HLT_j225_bloose | 0.999675 | 0.999843 | 0.999753 | 2.61512 |
| HLT_j175_bmedium | 1.07208 | 1.0365 | 1.05283 | 4.60289 |
| HLT_2j65_btight_j85 | 0.567637! | 0.73624! | 0.669779! | 31.4556 |
| HLT_7j45 | 0.86202! | 0.927897! | 0.89685! | 5.73062 |
| HLT_6j45 | 1.00967 | 1.00474 | 1.00721 | 3.17457 |
| HLT_5j85 | 0.970144 | 0.985646 | 0.977206 | 3.42981 |
| HLT_4j100 | 1.01543 | 1.00726 | 1.01181 | 2.14315 |
| HLT_3j175 | 1.02132 | 1.00972 | 1.01635 | 1.57934 |
| ”B-tagging” | 1.1138! | 1.05751 | 1.083 | 2.35134 |
| HLT_ht400 + ”B-tagging” | 1.1138! | 1.05751 | 1.083 | 2.35134 |
| HLT_ht550 + ”B-tagging” | 1.1138! | 1.05751 | 1.083 | 2.35134 |
| HLT_ht700 + ”B-tagging” | 0.987586 | 0.993821 | 0.99065 | 2.3796 |
| HLT_ht850 + ”B-tagging” | 0.944994 | 0.973187 | 0.957684 | 2.39551 |
| HLT_ht1000 + ”B-tagging” | 0.94873 | 0.975094 | 0.960507 | 2.39551 |

# 4 Summary and Interpretation

This study is a preliminary investigation of some triggers for use the in the Run-2 $W' \to tb$ hadronic final state analysis. We are interested in how some different triggers affect the acceptable $W'$ $m_{tb}$ range, and how they introduce bias into the ABCD method. We made a list of some single jet $p_T$ triggers, $H_T$ triggers, b-tag triggers, and multijet $p_T$ triggers that can be found in Table 1. In addition, we investigated the possibility of an $H_T$ + b-tag trigger by requiring an event pass a less restrictive b-tag requirement along with an $H_T$ trigger.

We generated efficiency curves for each trigger as a function of small-$R$ jet $p_T$, large-$R$ jet $p_T$, small-$R$ jet $H_T$, and large-$R$ jet $H_T$. These can be found in Appendix A. We determined the start of the trigger plateau region to be where 99% of events pass the trigger, and used this value to set a $p_T$ requirement on jets in the next part of the study, the ABCD method categorization. Events are categorized into four regions based on whether their large-$R$ jet passes the top-tagging requirement and/or their small-$R$ jet passes the b-tagging requirement. Events are categorized into one of the control regions (A, B, and C) if they one or both of these requirements, or into the signal region (D) if they pass both requirements. The control regions can then be used to estimate background contribution in the signal region. Comparisons of the $m_{tb}$ spectrum for events in region D to the ABCD method prediction can be found in Appendix B. Table 2 shows the values of $p_T$ where the trigger plateau region begins for both leading small-$R$ jet $p_T$ and leading large-$R$ jet $p_T$. Also listed is the determined minimum $m_{tb}$ value where this analysis is sensitive.

Finally, ratios between tagging efficiencies were calculated for events passing each trigger: $\frac{\varepsilon_{bt}}{\varepsilon_b \varepsilon_t}$, $\frac{\varepsilon_{b1}}{\varepsilon_{b2}}$, and $\frac{\varepsilon_{t1}}{\varepsilon_{t2}}$. These efficiency ratios were computed for the tagging requirements used in the $W' \to tb$ analysis and for randomized tagging requirements where both requirements are simply a 50% chance to tag. The coefficients for the real taggers are presented in Table 3 and for the random taggers in Table 4. These efficiency ratios provide insight into how biased the top-tag and b-tag requirements are when each trigger is applied. The ratios should be very close to 1 if the tagging requirements are unbiased.

As expected, the random tagging requirements show ratios close to 1 for every trigger except for one with low statistics. Since a randomized 50% chance to top-tag and b-tag should be completely unbiased, any deviation from 1 can be taken as the fractional uncertainty due to Monte Carlo statistics for that trigger. Under the actual top-tagging and b-tagging requirements:

**Single jet $p_T$ triggers and $H_T$ triggers**
: The ratios are all only a few percent off from 1, indicating that they do not introduce bias into the tagging requirements and are suitable for use in the $W' \to tb$Run-2 analysis.

**B-tag triggers**
: HLT_j300_bloose has reasonably high statistics and shows ratios only a few percent off from 1, making it worthy of further investigation. HLT_j300_bloose's ratios indicate that its application introduces a bias of about 20% into the tagging methods, making it unsuitable for use with the ABCD method. The HLT_j175_bmedium and HLT_2j65_btight_j85 triggers both have high statistical uncertainty, so conclusions can't be drawn about them from this study.

**Multijet triggers**
: HLT_7j45 has too high statistical uncertainty to draw conclusions about it from this study. The rest of the multijet triggers in general show efficiency ratios far departed from 1, indicating that they introduce bias into the tagging methods.

**Proposed $H_T$ + loose B-tag triggers**
: Efficiency ratios far from 1 indicate bias in the tagging ratios when these $H_T$ triggers and a loose b-tagging requirement are imposed on events.

It should be noted that the turn-on curves for the multijet triggers and $H_T$ + loose b-tagging proposed triggers are disfigured by the weighting scheme of the leading-parton-$p_T$ binned Monte Carlo samples. The start of the trigger plateau region may have therefore been incorrectly determined for these triggers, resulting in bias being introduced from the instability of the trigger outside of the plateau region. Further study is needed to determine the effect of the weighting on the trigger turn-on curve.

This study only examined QCD dijet background MC samples. In the near future, these triggers will be studied with $W'$ signal MC samples as well.

## Acknowledgements

This work was supported in part by the U.S. Department of Energy, Office of Science, Office of Workforce Development for Teachers and Scientists (WDTS) under the Science Undergraduate Laboratory Internships Program (SULI).

Argonne, a U.S. Department of Energy Office of Science laboratory, is operated under Contract No. DE-AC02-06CH11357.

# A Trigger Efficiency Curves

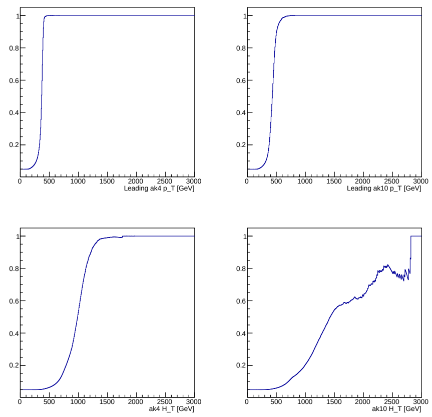


Figure A.1: HLT_j400 efficiency curves.

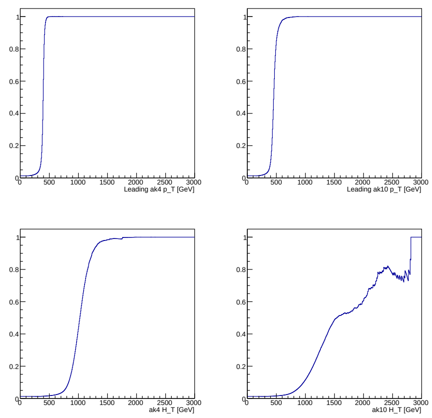


Figure A.2: HLT_j460 efficiency curves.

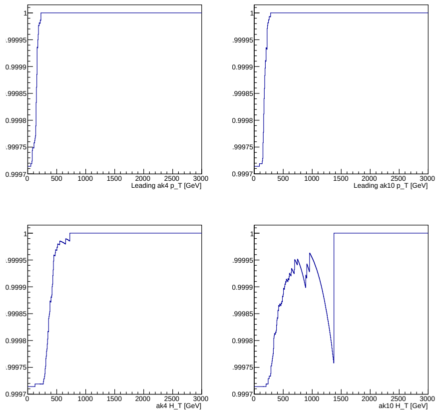


Figure A.3: HLT_j85 efficiency curves.

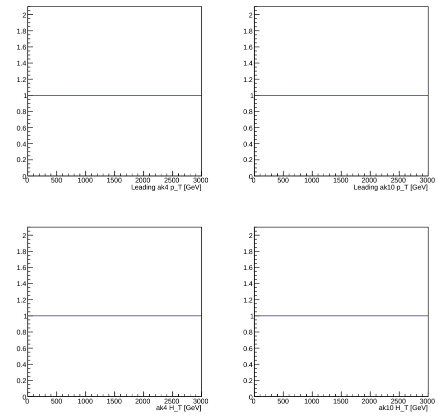


Figure A.4: HLT_j15 efficiency curves.

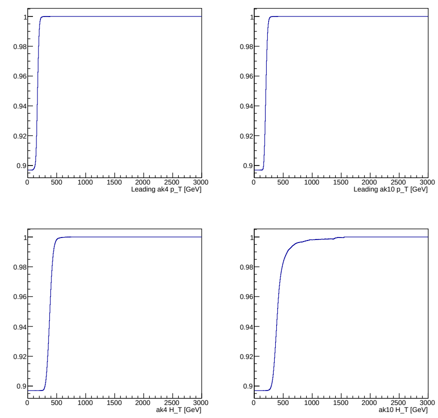


Figure A.5: HLT_ht400 efficiency curves.

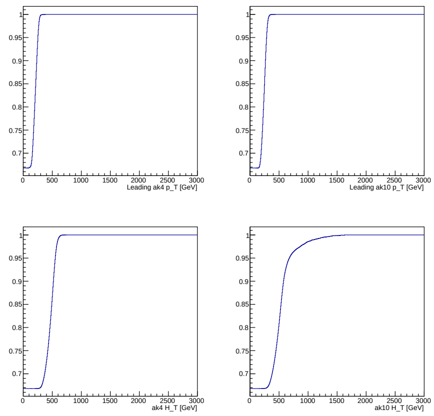


Figure A.6: HLT_ht550 efficiency curves.

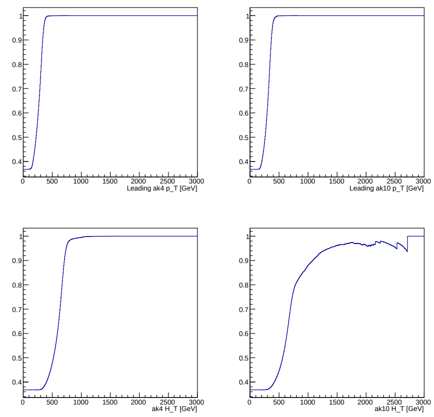


Figure A.7: HLT_ht700 efficiency curves.

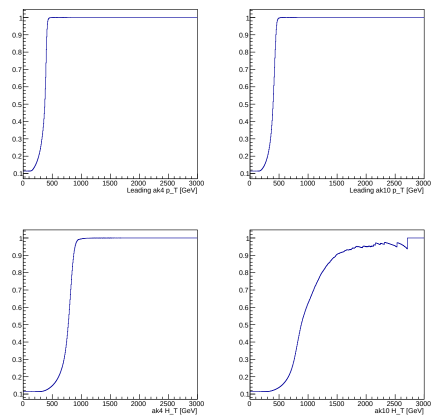


Figure A.8: HLT_ht850 efficiency curves.

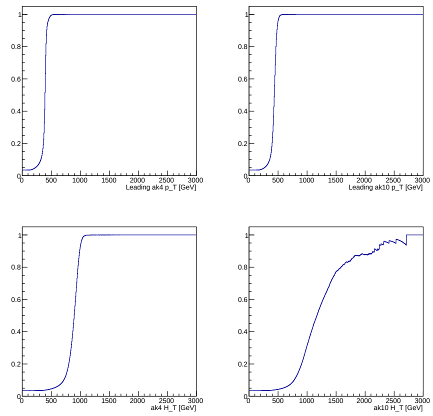


Figure A.9: HLT_ht1000 efficiency curves.

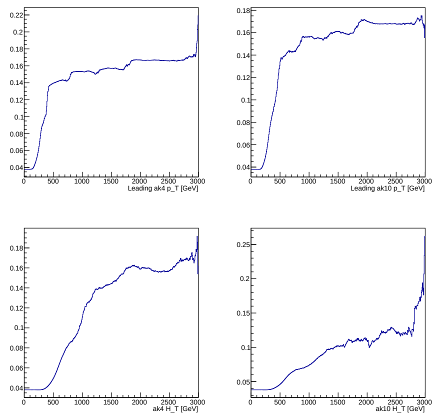


Figure A.10: HLT_j300_bloose efficiency curves.

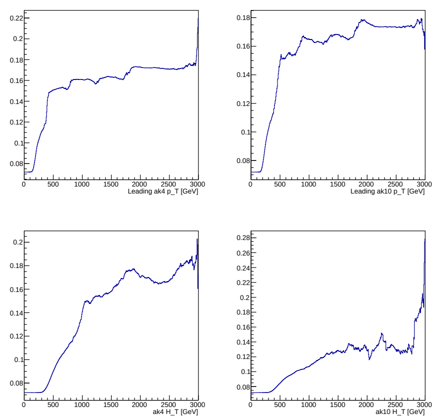


Figure A.11: HLT_j225_bloose efficiency curves.

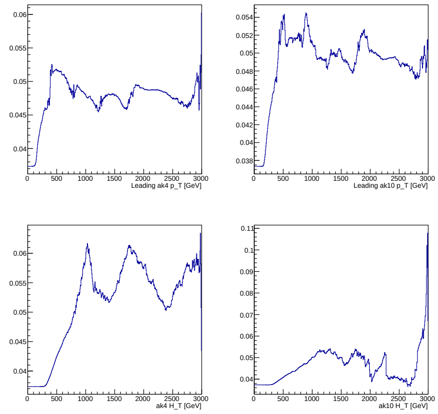


Figure A.12: HLT_j175_bmedium efficiency curves.

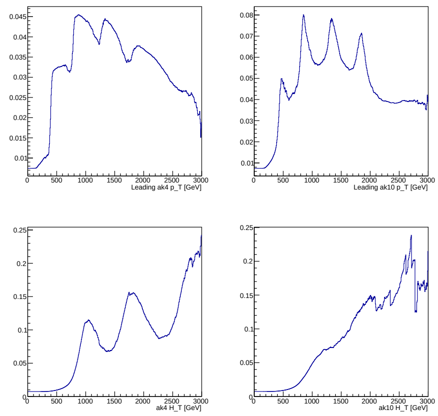


Figure A.13: HLT_7j45 efficiency curves.

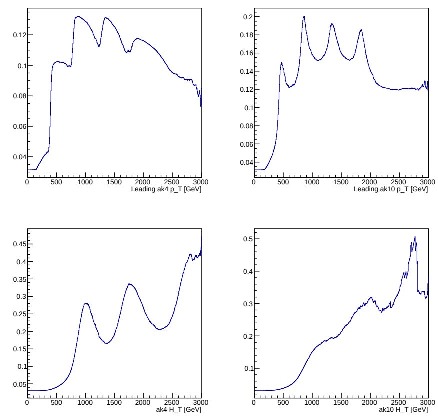


Figure A.14: HLT_6j45 efficiency curves.

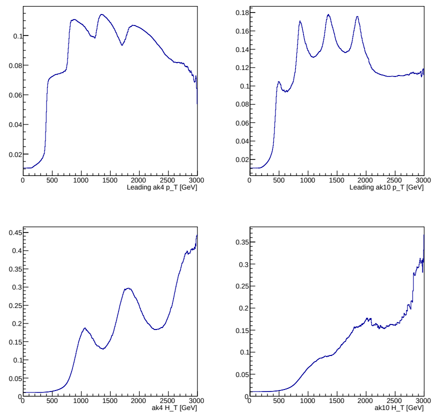


Figure A.15: HLT_5j85 efficiency curves.

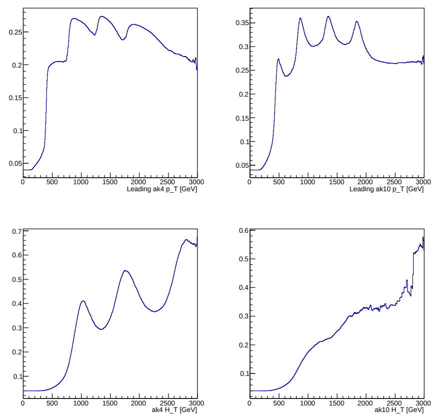


Figure A.16: HLT_4j100 efficiency curves.

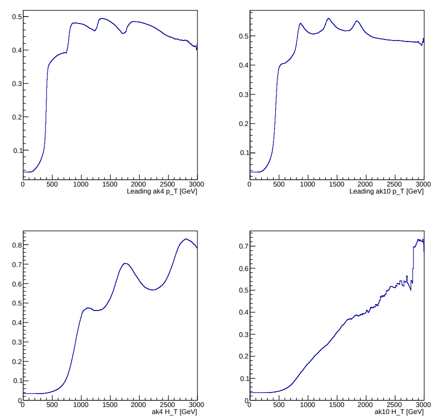


Figure A.17: HLT_3j175 efficiency curves.

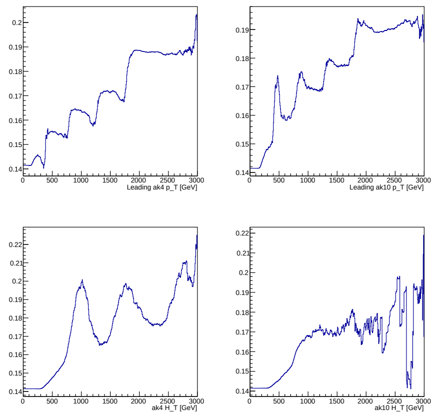


Figure A.18: "B-tag" efficiency curves.

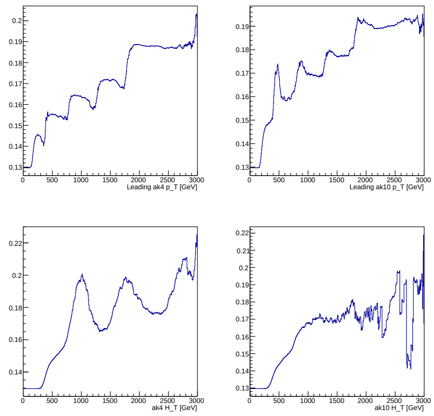


Figure A.19: HLT_ht400 + “B-tagging” efficiency curves.

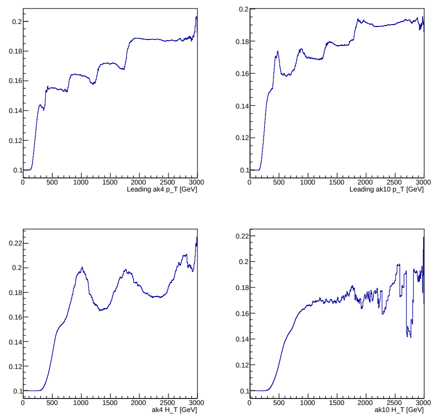


Figure A.20: HLT_ht550 + “B-tagging” efficiency curves.

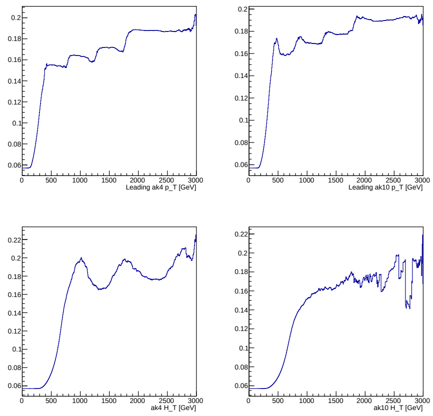


Figure A.21: HLT_ht700 + “B-tagging” efficiency curves.

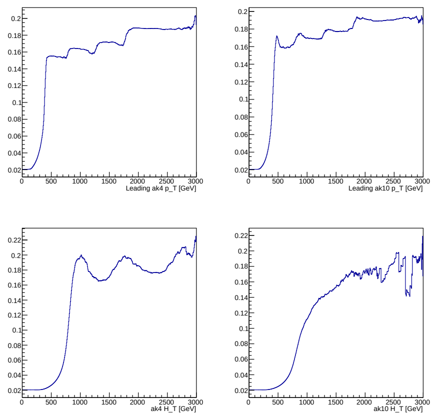


Figure A.22: HLT_ht850 + “B-tagging” efficiency curves.

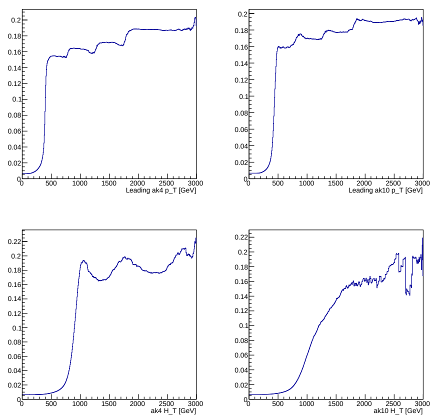


Figure A.23: HLT_ht1000 + “B-tagging” efficiency curves.

# B $m_{tb}$ Distributions, Actual vs. ABCD Method Prediction

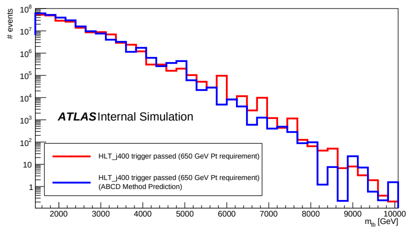


Figure B.1: HLT_j400 $m_{tb}$ distributions.

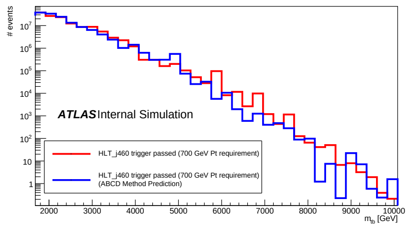


Figure B.2: HLT_j460 $m_{tb}$ distributions.

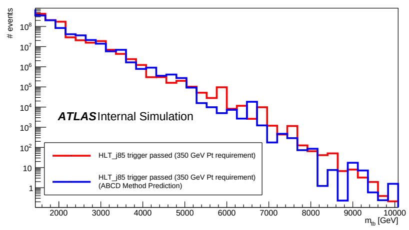


Figure B.3: HLT_j85 $m_{tb}$ distributions.

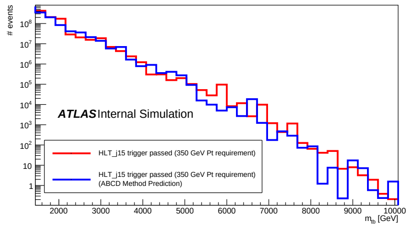


Figure B.4: HLT_j15 $m_{tb}$ distributions.

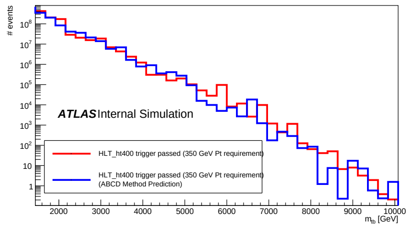


Figure B.5: HLT_ht400 $m_{tb}$ distributions.

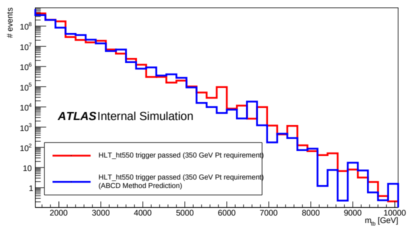


Figure B.6: HLT_ht550 $m_{tb}$ distributions.

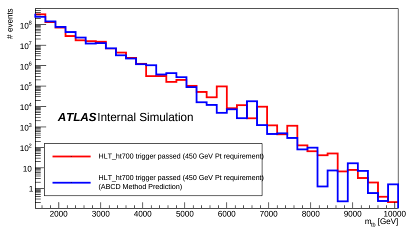


Figure B.7: HLT_ht700 $m_{tb}$ distributions.

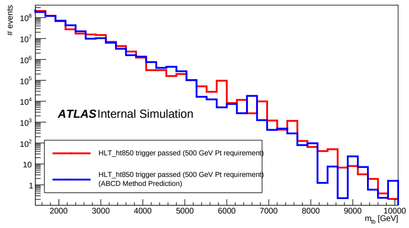


Figure B.8: HLT_ht850 $m_{tb}$ distributions.

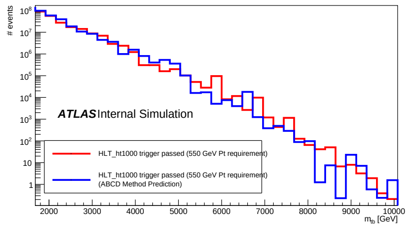


Figure B.9: HLT_ht1000 $m_{tb}$ distributions.

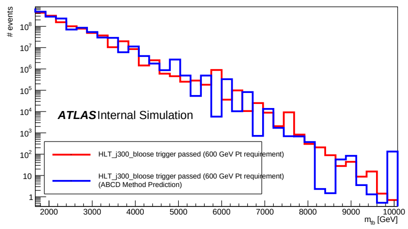


Figure B.10: HLT_j300_bloose $m_{tb}$ distributions.

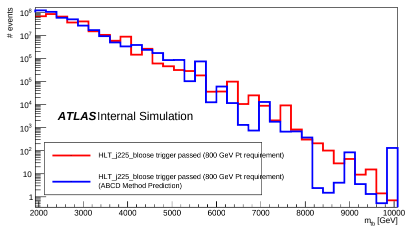


Figure B.11: HLT_j225_bloose $m_{tb}$ distributions.

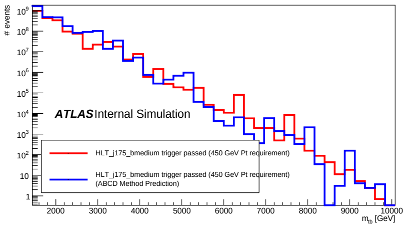


Figure B.12: HLT_j175_bmedium $m_{tb}$ distributions.

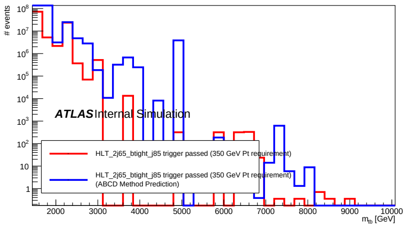


Figure B.13: HLT_2j65_btight_j85 $m_{tb}$ distributions.

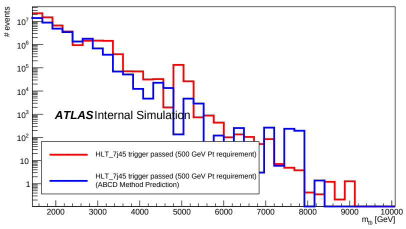


Figure B.14: HLT_7j45 $m_{tb}$ distributions.

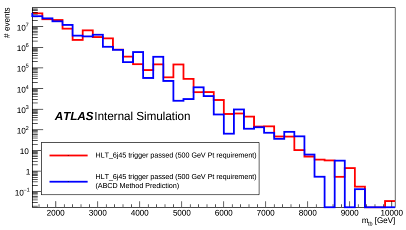


Figure B.15: HLT_6j45 $m_{tb}$ distributions.

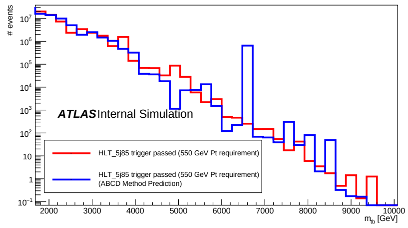


Figure B.16: HLT_5j85 $m_{tb}$ distributions.

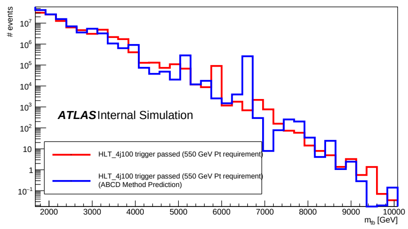


Figure B.17: HLT_4j100 $m_{tb}$ distributions.

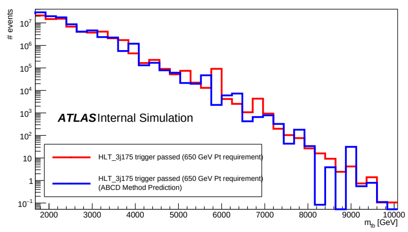


Figure B.18: HLT_3j175 $m_{tb}$ distributions.

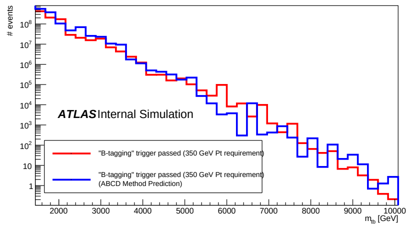


Figure B.19: “B-tag” $m_{tb}$ distributions.

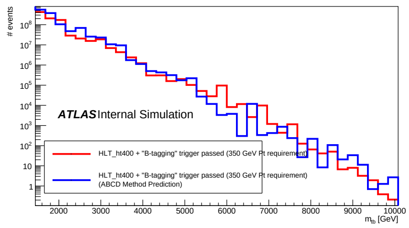


Figure B.20: “HLT_ht400 + B-tag” $m_{tb}$ distributions.

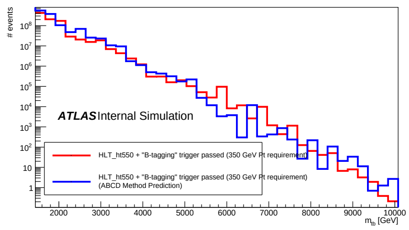


Figure B.21: “HLT_ht550 + B-tag” $m_{tb}$ distributions.

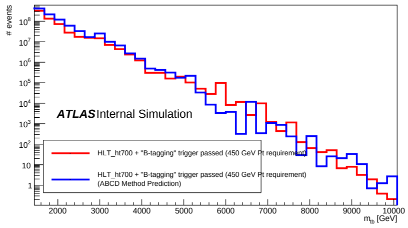


Figure B.22: "HLT_ht700 + B-tag" $m_{tb}$ distributions.

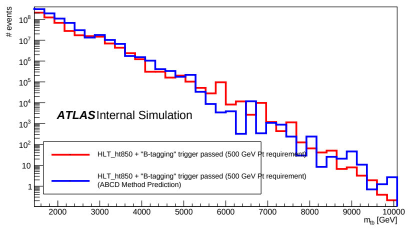


Figure B.23: "HLT_ht850 + B-tag" $m_{tb}$ distributions.

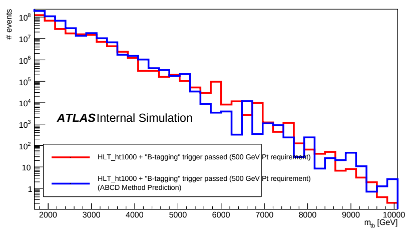


Figure B.24: "HLT_ht1000 + B-tag" $m_{tb}$ distributions.

## References


[1] ATLAS Collaboration, G. Aad et al., *Search for $W' \to t\bar{b}$ in the lepton plus jets final state in proton-proton collisions at a centre-of-mass energy of $\sqrt{s}$ = 8 TeV with the ATLAS Detector*, Physics Letters B **743** (2015) 235 – 255. http://dx.doi.org/10.1016/j.physletb.2015.02.051.

[2] ATLAS Collaboration, G. Aad et al., *Search for $W' \to tb \to qqbb$ Decays in pp Collisions at $\sqrt{s}$ = 8 TeV with the ATLAS Detector*, The European Physical Journal C **75** (2015) no. 4, 1434. http://dx.doi.org/10.1140/epjc/s10052-015-3372-2.

[3] J. Love, *Searching for Physics Beyond the Standard Model in the 3rd Generation with the ATLAS Detector*, Presentation, Mar, 2015. https://indico.hep.anl.gov/indico/conferenceDisplay.py?confId=586.